Stem Cell Research 41 (2019) 101617

Contents lists available at ScienceDirect

Stem Cell Research

journal homepage: www.elsevier.com/locate/scr

Immature mDA neurons ameliorate motor deficits in a 6-OHDA Parkinson's disease mouse model and are functional after cryopreservation

Dominique Leitner[a,b,c], Mahesh Ramamoorthy[a,b,c], Marion Dejosez[a,b,c], Thomas P. Zwaka[a,b,c,*]

[a] Department of Cell, Developmental, and Regenerative Biology, Mount Sinai Icahn School of Medicine, New York, NY 10029, United States
[b] Black Family Stem Cell Institute, Icahn School of Medicine at Mount Sinai, New York, NY 10029, United States
[c] Huffington Foundation Center for Cell-Based Research in Parkinson's Disease, Icahn School of Medicine at Mount Sinai, New York, NY 10029, United States

ARTICLE INFO

Key words:
Parkinson's disease
Cryopreservation
Midbrain dopaminergic neurons
Human induced pluripotent stem cells
6-OHDA mouse model

ABSTRACT

Parkinson's disease is associated with the loss of dopaminergic neurons in the midbrain. Clinical studies investigating replacement of these neurons with *in vitro*-generated neurons are currently underway. However, this approach has been limited by difficulties in scaling up on-demand production of midbrain dopaminergic (mDA) neurons from pluripotent stem cells. Cryo-preservation may offer a solution, as it allows for banking of quality controlled mDA neurons. In this study, we tested different freezing conditions and found that optimal cryopreservation of immature human mDA neurons at an early differentiation time point was achieved in STEM-CELLBANKER medium using a controlled freezing program.

1. Introduction

The early cell therapy trials for Parkinson's disease (PD) used material from fetal midbrains (Barker, 2014; Barker et al., 2013; Lindvall et al., 1992, 1990, 1989; Sawle et al., 1992). As fetal tissue is not readily available, new sources, including *in vitro*-differentiated neurons from pluripotent stem cells, have gained traction. Recent methodological advancements now allow pluripotent stem cells to be differentiated into neurons that are not unlike the dopaminergic cells found in the A9 nucleus of the substantia nigra, which represents the cell type affected in PD (McRitchie et al., 1996; Damier et al., 1999; Chung et al., 2005; Grealish et al., 2010; Kriks et al., 2011). Various improvements have been made to the existing protocols, including novel purification and transplantation strategies, as well as assays to test the extent to which *in vitro*-derived cells mimic the behavior of authentic neurons (Steinbeck and Studer, 2015; Studer, 2017; Sundberg and Isacson, 2014).

Unfortunately, the application of these new differentiation and transplantation techniques has been limited by difficulties in producing sufficient cells on demand. The cryopreservation of mass-produced and quality-controlled midbrain dopaminergic (mDA) neurons could offer an attractive solution for the limited availability of source material for research applications and potential therapies. To date, such cryogenic strategies have been established and tested only on day 33 of mDA differentiation or later (Wakeman et al., 2017). Transplantation of mDA neurons frozen at these stages typically results in low cell viability, meaning that high cell numbers are needed at the outset. mDA neurons that have differentiated for only 25 days *in vitro* appear to produce better results in experimental transplantation studies (Kriks et al., 2011; Steinbeck and Studer, 2015), but it is unclear how freezing mDA neurons at this early differentiation stage affects their viability, nor do we know what cell dose is needed for transplantation studies. Here, we tested various cryopreservation conditions to determine which method allows for recovery of the most functional mDA neurons.

2. Materials and methods

2.1. Cell culture

The human induced pluripotent stem cell line, TZ16 (hiPSTZ16; ISMMSi003-A) (Dejosez and Zwaka, 2017), was cultured in mTeSR (Stemcell Technologies, 85850) on growth factor-reduced Matrigel (Matrigel GFR, BD Biosciences, 354230). iCell DopaNeurons (Wakeman et al., 2017), which are commercially available mDA neurons frozen at 45 days of differentiation, were thawed and grown as recommended by the manufacturer (Cellular Dynamics International, DNC-301–030–001).

Abbreviations: 6-OHDA, 6-hydroxydopamine; hNA, human nuclear antigen; Hz, hertz; mDA, midbrain dopaminergic; MEA, multi-electrode array; n.s., not significant; PC, principal component; PD, Parkinson's disease; SCBanker, STEM-CELLBANKER freezing medium; TH, tyrosine hydroxylase

* Corresponding author at: Black Family Stem Cell Institute, One Gustave L. Levy Place, New York, NY 10028, United States.
E-mail address: thomas.zwaka@mssm.edu (T.P. Zwaka).

https://doi.org/10.1016/j.scr.2019.101617
Received 12 June 2019; Received in revised form 5 September 2019; Accepted 10 October 2019
Available online 24 October 2019

2.2. mDA differentiation

hiPSTZ16-IPS cells were differentiated into floor-plate midbrain dopaminergic (mDA) neurons following the previously described modified dual SMAD-inhibition-based floor plate (FP) induction protocol (Kriks et al., 2011; Steinbeck et al., 2015). Briefly, on day −1 of differentiation, iPS cells were plated onto Matrigel (BD Biosciences, 354230) at a density of 180,000 cells/cm^2 in the presence of 100 nM LDN193189 (Stemgent, 04–0074) and 10 μM SB431542 (Stemgent, 01–0010–50) for dual SMAD inhibition. This was followed by activation of the sonic hedgehog pathway with 100 ng/ml recombinant SHH protein (R&D Systems, 464-SH) and 2 μM purmorphamine (Calbiochem, 540220). After floor plate induction, cells were differentiated in the presence of 20 ng/ml BDNF (R&D Systems, 248-BD), 0.2 mM ascorbate (Sigma, A4034), 20 ng/ml GDNF (R&D Systems, 212-GD), 1 ng/ml TGF-β3 (R&D Systems, 243-B3-10), 0.5 mM dibutryl-cAMP (Sigma, D0627), and 10 μM DAPT (Tocris, 2634). On day 20, the cells were replated at 400,000 cells/cm^2 onto 15 μg/ml poly-L-ornithine (Sigma, 2634) containing 1 μg/ml laminin (Invitrogen, 23,017–015) and 2 μg/ml fibronectin (Sigma, F0895).

2.3. Immunocytochemistry

The expression of mDA differentiation markers was evaluated with immunocytochemistry. Cells were washed with Dulbecco's phosphate buffered saline (DPBS, Invitrogen, 14190250), fixed in 4% paraformaldehyde (Sigma, 158127), blocked for 1 h in 5% goat serum (Sigma, G9023) with 0.3% Triton x-100 (Sigma, T8787) at room temperature, and then incubated overnight at 4ºC with primary antibody in 1% BSA (Sigma, A2153) with 0.3% Triton X-100 (Sigma, T8787). Cells were washed three times with DPBS for 5 min, incubated with the secondary antibody and 1 μg/ml DAPI (Sigma, D9542) for 1 h at room temperature, and then mounted with Vectashield mounting medium (Vector Laboratories H-1200). The following antibodies were used at the indicated dilutions: anti-tyrosine hydroxylase (Pel-Freez, P40101-150; 1:100), anti-FOXA2 (Santa Cruz, sc-271103; 1:100), anti-TUBB1 (Biolegend, clone TUJ1, MMS-435P; 1:2000), AlexaFluor-594 goat anti-rabbit (Molecular Probes, A-11012; 1:200), and AlexaFluor-488 goat anti-mouse (A-11029, Molecular Probes; 1:200). Images were acquired on an inverted microscope, an Evos FL Cell Imaging System, or a Zeiss Axio Observer.Z1/7 at 20X magnification (LD Plan-Neofluar 20X/0.4 Korr Ph2 M27).

2.4. Electrophysiology

The electrophysiological profiles were determined with a multi-electrode array (MEA) plate (Axion Biosystems, M768-KAP-48). Forty-eight-well classic view MEA plates were coated with 0.07% polyethyleneimine (Sigma, 181978) and 80 μg/ml laminin (Invitrogen, 23017–015) according to the manufacturer's protocol. Neurons were dotted into wells at a density of 70,000 cells. Medium was changed every 2–3 days. A Maestro (Axion Biosystems) was used to record signals with a 200–4000 Hz Butterworth band filter at 37 °C, and the data were analyzed with the Axion 2.4 software. Spikes were processed with a 5.5 standard deviation detection limit.

2.5. Dopamine ELISA

As a functional parameter, the release of dopamine into the cell culture medium was measured under standard conditions and after KCl-stimulated depolarization (Steinbeck et al., 2015; Wakeman et al., 2017). Cells were plated onto 48-well MEA plates (Axion Biosystems, M768-KAP-48), washed with HBSS (Invitrogen, 14025–092) and then incubated with HBSS or HBSS + 55 mM KCl (Sigma, P9541) for 30 min at 37 °C. The supernatant was immediately frozen. Dopamine release was then measured by ELISA (Eagle Biosciences, DOU39-K01) according to the manufacturer's protocol and the dopamine concentration was determined with a 5-parameter logistical regression (MyAssays.com).

2.6. 6-Hydroxydopamine (6-OHDA) mouse model

Surgeries were performed according to NIH guidelines and approved by the Institutional Animal Care and Use Committee (IACUC) of Icahn School of Medicine at Mount Sinai. Eight-week-old male NOD-SCID IL2Rgc null (NSG) mice (005557, Jackson Laboratory) were lesioned by injection of 10 μg/2 μl 6-OHDA (Sigma, H116) into the right striatum at the coordinates (in millimeters) from bregma, AP (anteroposterior) +0.5, ML (mediolateral) +2.0, and DV (dorsoventral) −3.0 from dura, as described previously (Kriks et al., 2011; Steinbeck et al., 2015). Mice with successful lesions (as determined by the amphetamine-induced rotational assays described in Section 2.7) were put into three groups. Four weeks after 6-OHDA-induced lesioning, selected mice received either neuronal transplant or injection of neural differentiation medium into the right striatum at the coordinates (in millimeters), AP +0.5, ML +2.0 from bregma, and DV −3.2 from dura. The neuronal transplant involved experimental hiPSTZ16-mDA neurons on day 25 of differentiation or iCell DopaNeurons (see Section 2.1); transplants utilized 200,000 cells/2 μl of "D13+" neural differentiation medium. This medium, which was described by Kriks et al. (2011), included neurobasal medium (Invitrogen, 21,103,049), 1x B27 without retinoic acid (Invitrogen, 12,587–010), 3 μM CHIR99021 (Stemgent, 04–0004), 20 ng/ml BDNF (R&D Systems, 248-BD), 0.2 mM ascorbic acid (Sigma, A8960), 20 ng/ml GDNF (R&D Systems, 212-GD), 0.5 mM dbcAMP (Sigma, D0627), 1 ng/ml TGF-B3 (R&D Systems, 243-B3), and 10 μM DAPT (Tocris, 2634). Each group consisted of 6 mice.

2.7. Amphetamine-induced rotational behavioral test

Four weeks after 6-OHDA lesioning (see Section 2.6), the number of ipsilateral amphetamine-induced rotations (rotations toward the lesion on the right; clockwise) was quantified as described by Kriks et al. (2011). Mice were injected intraperitoneally with 10 mg/kg D-amphetamine (Sigma, A5880) and after 10 min, the rotational behavior was evaluated with the EthoVision XT system for 30 min. Mice that exhibited more than six rotations per minute, which is an indication of a massive loss of TH-positive neurons (more than 70%) following the 6-OHDA treatment (Iancu et al., 2005), were subjected to the transplantation assay described in Section 2.6. The rotational behavior was reassessed 4 and 8 weeks after transplant.

2.8. Immunolabeling-enabled imaging of solvent-cleared organs (iDISCO)

For histological evaluation of the grafts, mice were euthanized at 4 months post-transplant and transcardially perfused with DPBS followed by 4% paraformaldehyde (Sigma, 158127). The cerebellum was removed, the remaining brain tissue was bisected, incubated in 4% paraformaldehyde at 4 °C for 24 h, and then further processed as described previously (Renier et al., 2016, 2014). Briefly, samples were treated with methanol (Sigma, A412-4), permeabilized for 2 days, blocked for 4 days, exposed to primary antibodies against human nuclear antigen (hNA; Millipore, MAB1281; 1:200) and tyrosine hydroxylase (TH; Pel Freeze Biologicals, P40101-150; 1:100) for 4 days, and then exposed to secondary antibodies [AlexaFluor-680 (Molecular Probes, A-21084; 1:200) and AlexaFluor-594 (Molecular Probes, A-11012; 1:100)] for 4 days. The samples were cleared and imaged in dibenzyl ether (Sigma, 108014) using a light-sheet microscope (Ultramicroscope II, LaVision Biotec) equipped with an Andor Neo sCMOS camera and 4x/0.3 WD 6 LVMI-Fluor objective lens with a dipping cap (Rockefeller University). Images were captured using the following parameters: step size, 3 μm; gamma, 1.00; zoom, 0.63; laser width, NA 0.222; 640 nm laser power at

10%; and 561 nm laser power at 6%. The obtained images were rendered with the Imaris 9.0.2 software (Bitplane).

2.9. Cell freezing

Neurons were dissociated with Accutase (Invitrogen, AT-104) and frozen on day 24 of differentiation in either STEM-CELLBANKER (SCBanker, Amsbio, 11897) or mFreSR (Stemcell Technologies, 05855) freezing medium, at a density of 3–5 × 10^6 cells/ml. This density is typically used for cryopreservation of commercially available neurons (Cellular Dynamics International) and other cell types (Cohen et al., 2014). The cells were either frozen conventionally at a rate of 1°C/min using an isopropanol freezing container (Mr. Frosty, Nalgene) or with a controlled-rate freezer (Kryo10 Series II; Planer) running the following program (Wong et al., 2017): Step 1: 4°C; Step 2: 1.2°C/min to −4°C; Step 3: 25°C/min to −40°C; Step 4: 10°C/min to −12°C; Step 5: 1.0°C/min to −40°C; Step 6: 10°C/min to −90°C; Step 7: wait at −90 °C. Once the controlled-rate freezer reached −90°C, the cryotubes were rapidly transferred to a liquid nitrogen tank. Neurons were frozen for 4 weeks before being thawed onto dishes coated with 15 μg/ml poly-L-ornithine, 1 μg/ml laminin, and 2 μg/ml fibronectin, at 400,000 cells/cm^2. Thawing was performed rapidly at 37 °C.

2.10. RNAseq

On day 30 of differentiation, total RNA was extracted from hiPSTZ16-mDA neurons using the RNeasy kit and DNAse treatment (Qiagen, 74104) according to the manufacturer's protocol. Libraries were created with the NEBNext Poly(A) mRNA magnetic isolation module (New England Biolabs, E7490S), following the manufacturer's protocol. We used 0.5–1.0 μg total RNA, NEBNext Sample Purification Beads (New England Biolabs, E7765S), and NEBNext Multiplex Index primers (New England Biolabs, E7335S). Samples were evaluated on a Bioanalyzer, pooled, and sequenced by the Mount Sinai Genomics Core Facility on an Illumina HiSeq 4000. STAR aligner was used to map the reads to the Homo Sapiens UCSC genome using the hg19 genome and annotation data from the following link: http://cole-trapnell-lab.github.io/cufflinks//igenome_t able/index.html. The data were normalized by reads per kilobase of transcript per million mapped reads (RPKM) normalization. After normalization, genes were removed from the total list of genes if they had zero expression across all samples or if they had an average normalized expression below 1.5.

3. Results

3.1. mDA neuron differentiation and functional testing of the iPSTZ16 cell line

We first tested whether our human induced pluripotent stem (iPS) cell line hiPSTZ16 (Dejosez and Zwaka, 2017) is capable of differentiating into mDA neurons. Using a floor plate-based protocol (Kriks et al., 2011), hiPSTZ16-mDA neurons were differentiated (see Section 2.2) and characterized by testing mDA marker expression and morphology at different time points (see Section 2.3). On day 23 of differentiation, early hiPSTZ16-mDA neurons with extended processes were found to express tyrosine hydroxylase (TH, the rate-limiting enzyme of dopamine synthesis), FOXA2 (a floor-plate marker), and TUBB1 (tubulin beta 1 class VI, a neuronal marker detected by the TUJ1 antibody) (Fig. 1A). Expression of all three markers was retained at day 50 of differentiation (Fig. 1B). Morphologically, hiPSTZ16-mDA neurons at this stage formed cellular hubs and became interconnected by processes, reflecting the increasing complexity of the growing network.

We then tested the functionality of hiPSTZ16-mDA neurons *in vitro* by performing electrophysiological profiling and assessing their ability to release dopamine, and *in vivo* using the 6-hydroxydopamine (6-OHDA) PD mouse model (Kriks et al., 2011; Tieu, 2011).

In vitro, the electrophysiological profile acquired using a multi-electrode array (MEA, Section 2.4) indicated that hiPSTZ16-mDA neurons were electrically active on day 50 of differentiation, and that they exhibited a regular firing pattern at this time point (Fig. 1C). The secretion of dopamine into the cell culture medium, which indicates successful mDA neuron differentiation (Steinbeck et al., 2015; Wakeman et al., 2017), was 0.97 ng/ml on day 50 of differentiation and was further increased to 1.61 ng/ml upon depolarization with KCl (Fig. 1D) as measured by ELISA (see Section 2.5). Although this increase did not attain statistical significance, it is indicative of mDA neuron functionality, as previously reported (Wakeman et al., 2017).

To test functionality *in vivo*, we transplanted hiPSTZ16-mDA neurons into the striatum of 6-OHDA lesioned mice (Fig. 1E), which provide a mouse model for PD (see Section 2.6). At 4 weeks post-lesioning, we assessed the effect of transplantation on amphetamine-induced behavioral rotation (see Section 2.7). Mice that exhibited more than 6 rotations per minute (RPM) were injected with neurons or neural differentiation medium into the ipsilateral striatum, and their rotational behavior was tested at 4 and 8 weeks after transplantation. Control mice that received neural differentiation medium alone maintained an average of 15 RPM over the course of the study (Fig. 1F), indicating the persistence of an ipsilateral striatal lesion. However, the amphetamine-induced rotation of mice that received hiPSTZ16-mDA neurons at day 25 of differentiation was decreased to 5 RPM by 8 weeks post-transplantation. These results, which suggest that the *in vitro*-differentiated hiPSTZ16-mDA neurons are functional, is similar to results obtained with cryopreserved commercially available iCell DopaNeurons at day 45 of differentiation. Interestingly, the hiPSTZ16-mDA neurons reduced the RPM ~1.5-fold more than transplantation of iCell DopaNeurons. Four months after transplantation, the histology of the graft was evaluated by immunolabeling-enabled 3D imaging of solvent-cleared organs (iDISCO), as described in Section 2.8 (Renier et al., 2014). Using an antibody against human nuclear antigen (hNA), we were able to identify transplanted hiPSTZ16-mDA neurons that colocalized with the dopaminergic marker TH, in the striatum (Fig. 1G). Our results indicate that hiPSTZ16-mDA neurons survive and are functionally capable of correcting the motor deficit induced by 6-OHDA.

3.2. Viability and transcriptome of cryopreserved mDA neurons

In our effort to generate cryopreserved stocks of mDA neurons for cell replacement therapy, we set out to evaluate several methods of cryopreservation to determine which technique produces the most functional mDA neurons. We tested two different chemically defined freezing media, mFreSR and STEM-CELLBANKER (SCBanker) in combination with different freezing rates using conventional freezing containers or a controlled freezer (see Section 2.9 for details). hiPSTZ16-mDA neurons were frozen on day 24 of differentiation and thawed 4 weeks later. This time point would be optimal for both *in vivo* transplant and *in vitro* applications and has been shown to produce functional neurons after transplantation *in vivo* (Kriks et al., 2011; Steinbeck et al., 2015)

Trypan blue dye-exclusion tests performed at the time of thawing indicated that the viability of neurons frozen in SCBanker with a cryogenic freezing container or in a controlled freezer was 71% and 78%, respectively (Fig. 2A), whereas the use of mFreSR yielded slightly lower viabilities of 55% and 64%, respectively. Overall, the freezing conditions did not significantly differ in terms of viability.

RNAseq analysis of both non-frozen and thawed hiPSTZ16-mDA neurons on day 30 of differentiation (see Section 2.10) followed by principal component analysis (PCA) revealed that all samples showed similar transcriptional profiles. Additionally, we found that cells frozen at different freezing rates clustered together dependent on the freezing medium. This indicates that, relatively, the freezing medium induced transcriptional changes to a higher degree than the freezing rate. We then compared the expression levels of selected markers that are

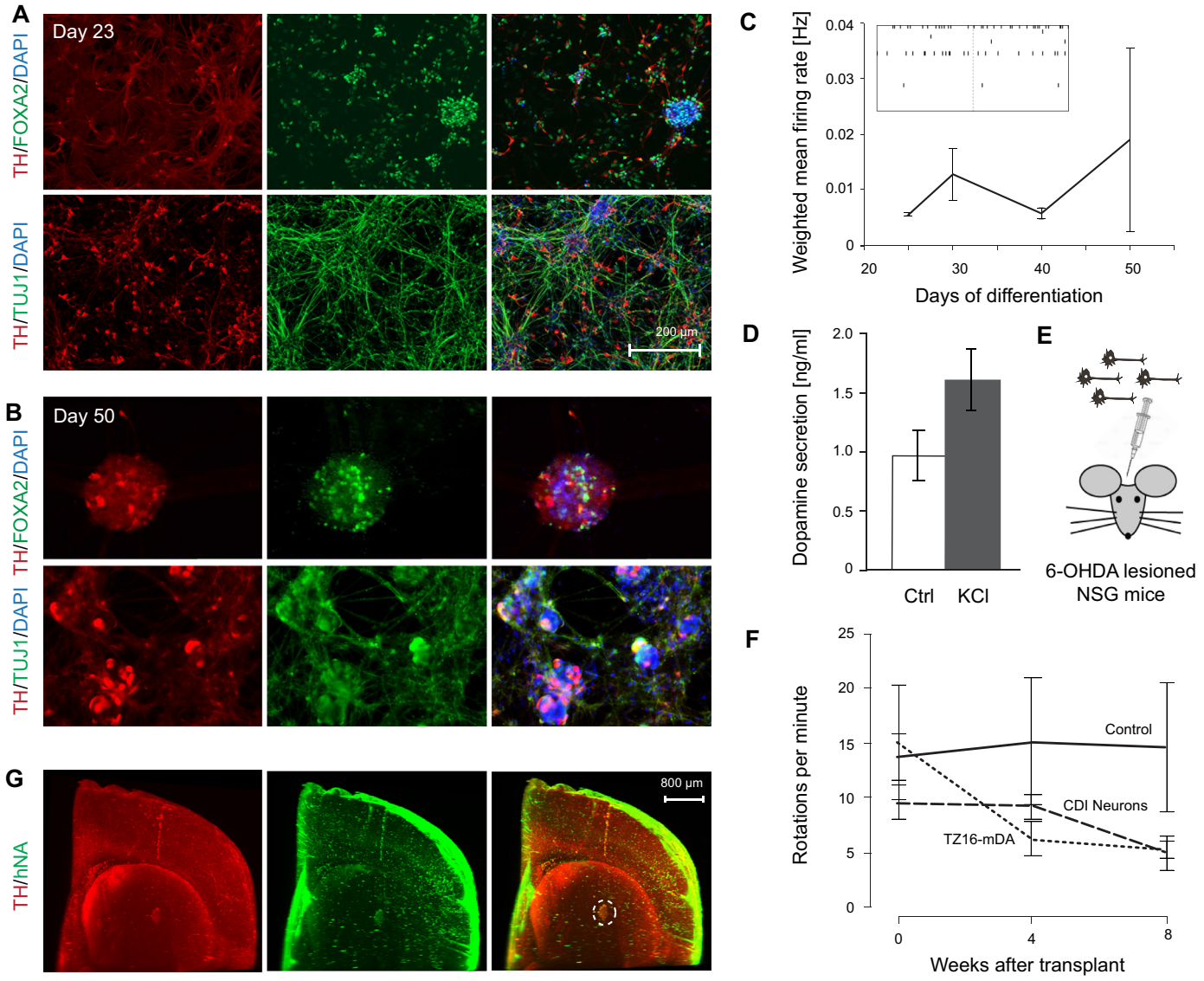

Fig. 1. Midbrain dopaminergic neuron characterization *in vitro*, and *in vivo* with the 6-OHDA Parkinson's disease animal model. hiPSTZ16-IPS cells were differentiated into mDA neurons and analyzed for expression of the indicated markers, on (A) day 23 and (B) day 50 of differentiation. (C) Weighted mean firing rate of hiPSTZ16-mDA cells at the indicated days of differentiation, as measured using multi-electrode arrays. The insert presents raster plots of bursting cultures assessed for a period of 1 min on day 50 of differentiation. (D) Measurement of dopamine secretion into the cell culture medium on day 50 of differentiation without and with KCl stimulation. Data are shown as the mean ± SEM of biological triplicates. (E) Illustration of *in vitro*-differentiated neuron injection into the striatum of NSG mice. (F) Amphetamine-induced rotational behavior 8 weeks after transplantation of the indicated cell types into the right striatum of NSG mice injected with 6-OHDA. Data represent the mean ± SEM; $n = 6$ per group. (G) Neurons in lesioned striatum 4 months after hiPSTZ16-mDA neuron transplant, visualized using iDISCO. A snapshot of a 3D image is shown. The dashed circle surrounds the area of injected neurons that were positive for TH and hNA.

relevant to mDA neuron differentiation between the different freezing conditions and non-frozen neurons (that mature into functional mDA neurons *in vivo*, Fig. 1C-F) (Fig. 2C). Specifically, our iPS-derived neurons expressed FOXA2, OTX2, and LMX1A above background levels, indicating midbrain floor plate characteristics, whereas forebrain regional markers, such as FOXG1, or markers of other neuronal subtypes (e.g., DBH, VGlut1, CHAT, and OLIG2) were not expressed. On the other hand, dopaminergic markers TH, NURR1, GIRK2, PTX3, DRD2, VMAT2, and AADC were expressed equally in frozen or non-frozen iPS-derived neurons. This expression profile is overall similar to that seen in the human substantia nigra (Wakeman et al., 2017), but the low expression levels of EN1 and some of the dopaminergic markers indicate that the mDA neurons were in an immature state at the analyzed time point.

3.3. Functionality of cryopreserved mDA neurons

Next, we evaluated the morphology of thawed hiPSTZ16-mDA neurons, their expression of mDA neuron markers, and several parameters of functionality across all cryopreservation conditions.

On the first day post-thaw, the morphology of hiPSTZ16-mDA neurons was similar across all conditions (Fig. 3A). By day 30 of differentiation, morphological analyses indicated that the neurons had started to form cell clusters that were interconnected by processes (Fig. 3B). At this time point, thawed hiPSTZ16-mDA neurons expressed FOXA2 (Fig. 3C), TUBB1 (detected with TUJ1 antibody) (Fig. 3D), and TH. In addition, cellular clusters and processes connecting these clusters were apparent. These changes were observed across all cryopreservation conditions with no apparent differences.

To establish an electrophysiological profile, we evaluated hiPSTZ16-mDA neurons using a multi-electrode array (MEA) beginning

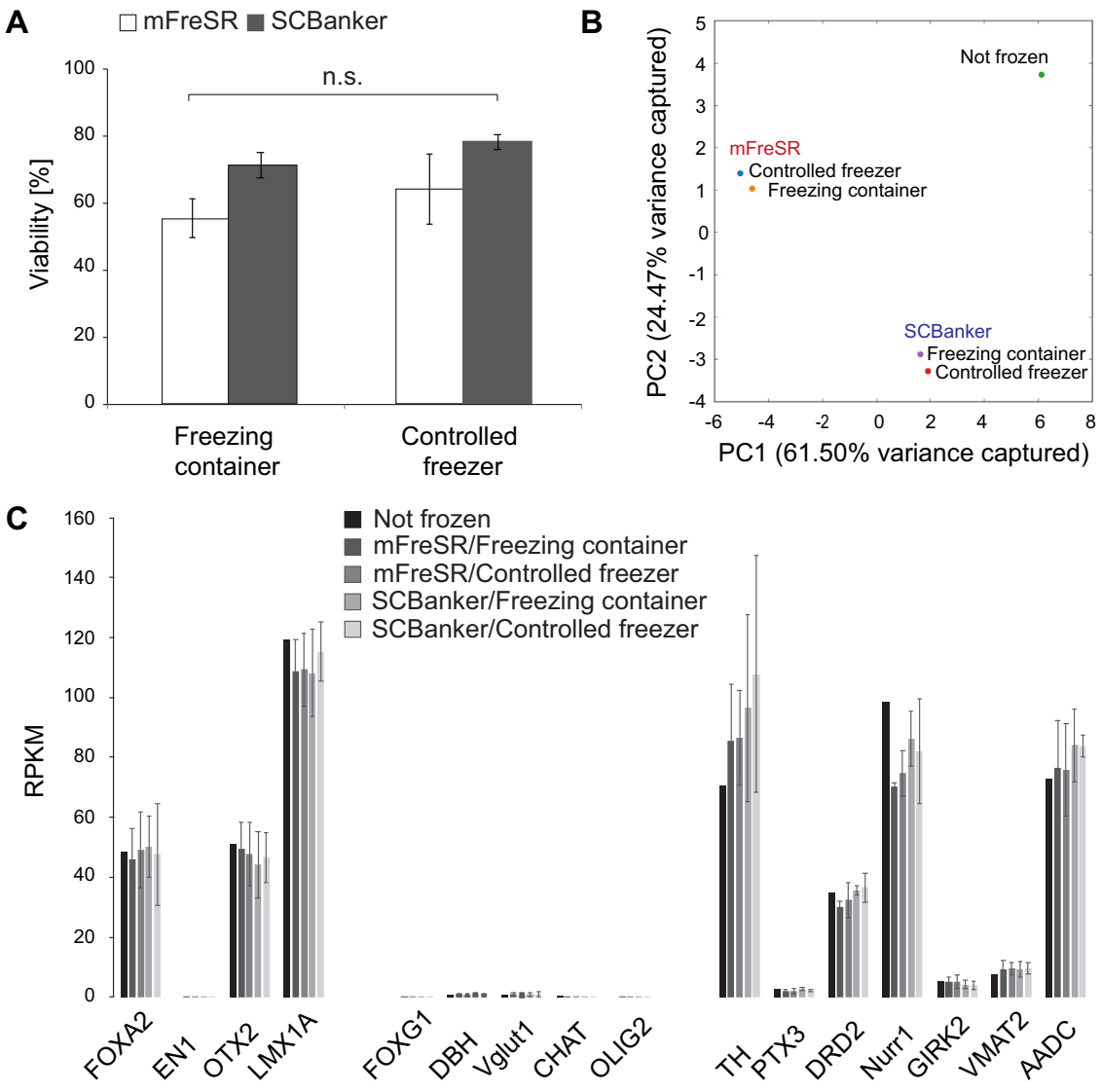

Fig. 2. Cryopreserved mDA neuron viability and transcriptome. (A) The trypan blue exclusion assay was used to measure the viability of hiPSTZ16-mDA neurons that were cryopreserved on day 24 of differentiation at the indicated conditions and thawed 4 weeks later. Data represent the mean ± SEM; $n = 3$. There was no significant difference across the freezing conditions. (B) RNASeq and Principle Component analyses of cryopreserved hiPSTZ16-mDA neurons on day 30 of mDA differentiation in comparison with neurons that were not frozen. (C) RPKM (reads per kilobase of transcript per million mapped reads) values of indicated markers as determined in RNAseq analyses of cryopreserved mDA neurons ($n = 2$) in comparison with control cells that were not frozen. Data are shown as mean ± SD.

2 days after thawing (day 26 of differentiation) and additional time points until the neurons reached maturity (days 30, 40 and 50). The neurons that exhibited the highest firing rate on day 50 of differentiation were those frozen in mFreSR using a standard freezing container, or in SCBanker using a controlled freezer (Fig. 4A, B).

Finally, to complement our assessment of electrical activity as a measure of functionality, we evaluated the secretion of dopamine into the cell culture medium on day 50 of differentiation. We found that the highest level of dopamine secretion came from hiPSTZ16-mDA neurons frozen in SCBanker using a controlled freezer (Fig. 4C).

4. Discussion

In this study, we investigated optimal methods for cryopreserving mDA neurons as a strategy for producing cells that maintain their functionality and are available on demand. First, the iPS cell line, hiPSTZ16 (Dejosez and Zwaka, 2017), was differentiated into mDA neurons and characterized *in vitro* and *in vivo*. Differentiated hiPSTZ16-mDA neurons expressed the previously described mDA markers (Kriks et al., 2011) and were functional, as determined by their electrophysiological profile and dopamine secretion. When transplanted *in vivo*, these neurons promoted functional recovery in the 6-OHDA mouse model, exhibiting a faster recovery rate than that attained using commercially available iCell DopaNeurons.

To date, cryopreservation has been evaluated in a broad range of cell types and applications, including primary neurons (Higgins et al., 2011), *in vitro* fertilization (IVF) (Rienzi et al., 2010), bone marrow cell transplants (Yang et al., 2003), and stem cells (Holm et al., 2010; Wong et al., 2017). For each of these applications/cell types, viability and functionality have been optimized by investigating the freezing rate and freezing media.

The freezing rate is a particularly important variable, as it has been shown that cell injury is more likely at both very low and very high cooling rates (Elliott et al., 2017). Slower cooling increases osmotic stress because it results in greater loss of water from the cell and less intracellular ice formation. Faster cooling leads to the formation of more intracellular ice, because water does not migrate out of the cell. Cryopreservation in a controlled-rate freezer removes water from the

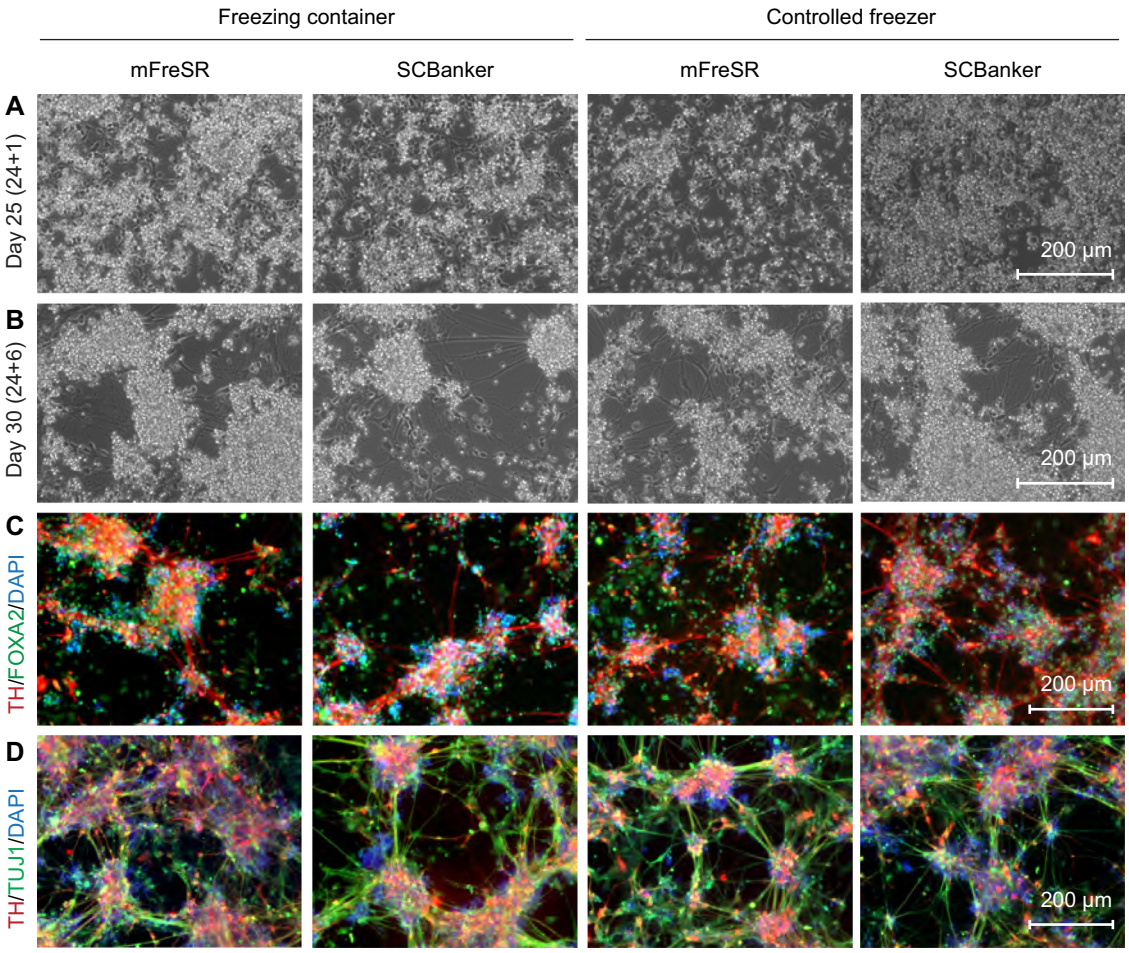

Fig. 3. Morphology and marker expression of cryopreserved mDA neurons. (A) hiPSTZ16-mDA neurons were frozen under the indicated conditions and morphology was assessed 1 day and (B) 5 days after thawing. (C, D) Evaluation of marker expression on day 30 of differentiation.

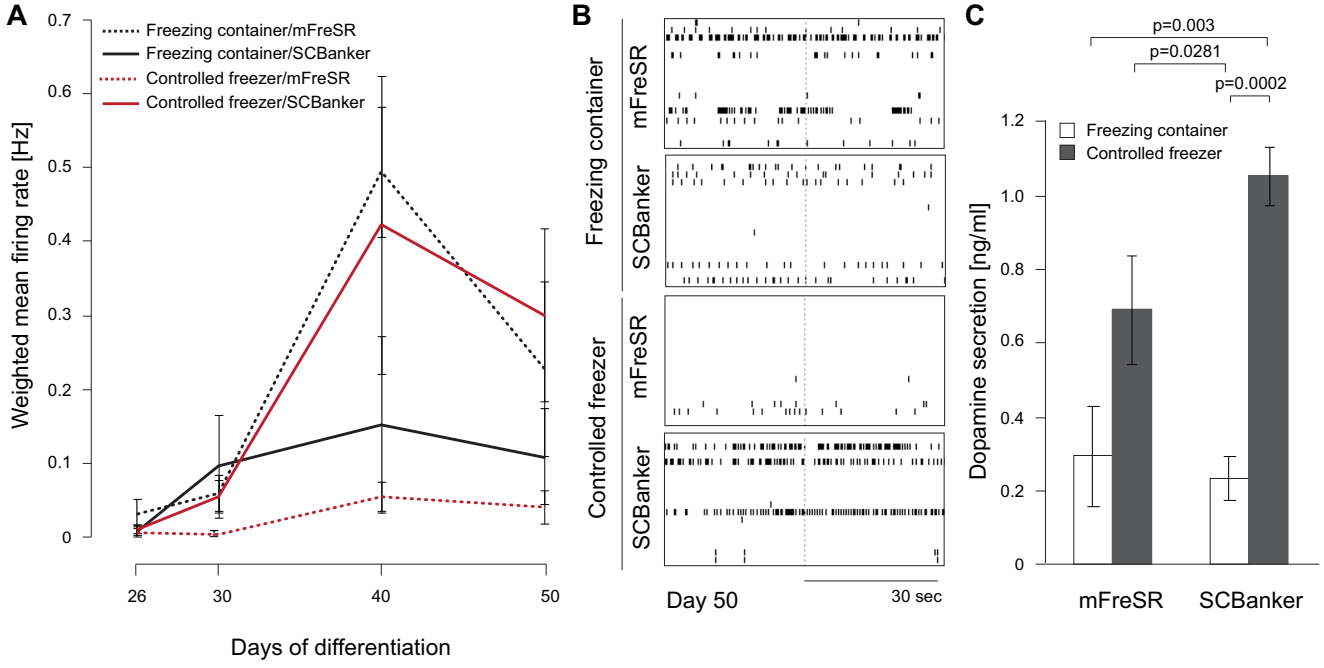

Fig. 4. Cryopreserved mDA neuron functionality. (A) The weighted mean firing rate was measured in cryopreserved hiPSTZ16-mDA neurons 2 days after they were thawed and plated (day 26 of differentiation) and at days 30, 40 and 50 of differentiation. (B) Raster plots are shown for each cryopreservation condition on day 50 of differentiation. (C) Dopamine secretion from cryopreserved hiPSTZ16-mDA neurons on day 50 of differentiation, as measured by ELISA. Data are presented as mean ± SEM; $n = 4$.

cells and freezes the cells at a rapid cooling rate. The cooling rate tested previously with mDA neurons was 1 °C/min to −60 °C, followed by 10 °C/min to −100 °C, which is similar to the rate obtained using conventional methods and an isopropanol container (Wakeman et al., 2017).

The components of the freezing medium have also been extensively evaluated, because they impact post-thaw viability through osmolarity effects and ice formation during freezing (Elliott et al., 2017). Cryoprotectants in the freezing medium can cause freezing-point depression and promote greater dehydration of cells prior to intracellular freezing. Additionally, both cell-permeating and non-permeating cryoprotectants are available; the latter includes high-molecular-weight cryoprotectants like sugars, which form polymers that stabilize the outside of cells. Dimethyl sulfoxide (DMSO) is a cell-permeable, small-molecular-weight cryoprotectant that is found in many freezing media; it can sustain the cell membrane by interacting with the polar head groups of phospholipids within the lipid bilayer. Here, we tested mFreSR and SCBanker, two chemically defined serum-free freezing media that contain DMSO and are similar to CryoStor, which was previously used in the freezing of mDA neurons (Wakeman et al., 2017). We chose mFreSR because it is one of the most commonly used stem cell freezing media, and we chose SCBanker because it contains anhydrous dextrose as an additional cryoprotectant and was recently deployed to cryopreserve and bank human pluripotent stem cells in single-cell, ready-to-use aliquots that showed high post-thaw viability (Wong et al., 2017).

By testing various combinations of freezing rates and freezing media, we evaluated the viability and functionality of cryopreserved hiPSTZ16-mDA neurons at a differentiation time point that is optimal for subsequent *in vivo* and *in vitro* assays. The viability of neurons frozen in SCBanker was similar when we used a standard cryogenic container (71%) or a controlled freezer (78%). These values are comparable to, if not greater than, the values previously reported for mDA neurons frozen at a later point in differentiation (Wakeman et al., 2017).

We also evaluated the transcriptome of hiPSTZ16-mDA neurons several days after thawing. Our results revealed that neurons frozen in SCBanker were most similar to non-frozen neurons, regardless of the utilized freezing rate. None of the freezing conditions appeared to impact the morphology or mDA marker expression of neurons at day 30 of differentiation. By day 50 of differentiation, neurons cryopreserved in a controlled freezer with SCBanker or in a cryogenic container with mFreSR showed the highest electric activity, and those frozen using the controlled freezer exhibited the highest level of dopamine release. Although it is possible that optimal freezing conditions might vary between cell lines, a pilot study performed with H9 ES cells revealed that those frozen in SCBanker at a controlled rate on day 24 of mDA differentiation also showed the highest viability after thawing and the highest dopamine secretion level at day 50 of differentiation. Taken together, our data indicate that mDA neurons frozen on day 24 of differentiation in SCBanker using a controlled freezer produce the most functional neurons.

It is widely acknowledged that most of the observed freezing-related constraints are imposed on frozen cells during the freezing process itself, and the recovery rate remains largely unaltered after longer storage periods (Miyamoto et al., 2018). Hence, we do not expect that long-term storage will affect the viability and functionality of mDA neurons differentially with regards to the utilized freezing method. Future studies will show if this is, indeed, the case.

Funding

This research was supported by the Huffington Foundation.

Author declaration

We wish to confirm that there are no known conflicts of interest associated with this publication and there has been no significant financial support for this work that could have influenced its outcome.

Declaration of Competing Interest

The authors declare no conflicts of interest.

Acknowledgments

We would like to acknowledge the Genomics Core Facility at Mount Sinai and the Rockefeller University Bioimaging Resource Center. We also thank the Zhenyu Yue laboratory (Yuanxi Zhang) at Mount Sinai for assistance with the PD mouse model, the Lorenz Studer laboratory (Sonja Kriks and Julius Steinbeck) at Memorial Sloan Kettering for discussions about neuron differentiation and the PD mouse model, and the Marc Tessier-Lavigne laboratory (Nicholas Renier) at the Rockefeller University for technical assistance with the iDISCO.

References

Barker, R.A., 2014. **Developing stem cell therapies** for **Parkinson's disease**: **waiting until** the **time** is **right**. Cell Stem Cell 15 (5), 539–542. https://doi.org/10.1016/j.stem.2014.09.016.

Barker, R.A., Barrett, J., Mason, S.L., Björklund, A., 2013. Fetal dopaminergic transplantation trials and the future of neural grafting in Parkinson's disease. Lancet Neurol. 12, 84–91. https://doi.org/10.1016/S1474-4422(12)70295-8.

Chung, D.Y., Seo, H., Sonntag, K.C., Books, A., Lin, L., Isacson, Q., 2005. Cell type-specific gene expression of midbrain dopaminercig neurons reveals molecules involved in their vulnerability and protection. Hum. Mol. Genet. 14, 1709–1725.

Cohen, R.I., Thompson, M.L., Schryver, B., Ehrhardt, R.O., 2014. Standardized cryopreservation of pluripotent stem cells. Curr. Protoc. Stem Cell Biol. 28 Unit 1C.14.

Damier, P., Hirsch, E.C., Agid, Y., Graybiel, A.M., 1999. The substantia nigra of the human brain. II. Patterns of loss of dopamine-containing neurons in Parkinson's disease. Brain 122, 1437–1438.

Dejosez, M., Zwaka, T.P., 2017. Generation of hiPSTZ16 (ISMMSi003-A) cell line from normal human foreskin fibroblasts. Stem Cell Res. 26, 44–46. https://doi.org/10.1016/j.scr.2017.11.019.

Elliott, G.D., Wang, S., Fuller, B.J., 2017. Cryoprotectants: a review of the actions and applications of cryoprotective solutes that modulate cell recovery from ultra-low temperatures. Cryobiology 76, 74–91. https://doi.org/10.1016/j.cryobiol.2017.04.004.

Grealish, S., Jönsson, M.E., Li, M., Kirik, D., Björklund, A., Thompson, L.H., 2010. The A9 dopamine neuron component in grafts of ventral mesencephalon is an important determinant for recovery of motor function in a rat model of Parkinson's disease. Brain 133, 482–495.

Higgins, A.Z., Cullen, D.K., LaPlaca, M.C., Karlsson, J.O., 2011. Effects of freezing profile parameters on the survival of cryopreserved rat embryonic neural cells. J. Neurosci. Methods 201, 9–16. https://doi.org/10.1016/j.jneumeth.2011.06.033.

Holm, F., Ström, S., Inzunza, J., Baker, D., Strömberg, A.M., Rozell, B., Feki, A., Bergström, R., Hovatta, O., 2010. An effective serum- and xeno-free chemically defined freezing procedure for human embryonic and induced pluripotent stem cells. Hum. Reprod. 25, 1271–1279. https://doi.org/10.1093/humrep/deq040.

Iancu, R., Mohapel, P., Brundin, P., Paul, G., 2005. Behavioral characterization of a unilateral 6-OHDA-lesion model of Parkinson's disease in mice. Behav. Brain Res. 162 (1), 1–10. https://doi.org/10.1016/j.bbr.2005.02.023.

Kriks, S., Shim, J.W., Piao, J., Ganat, Y.M., Wakeman, D.R., Xie, Z., Carrillo-Reid, L., Auyeung, G., Antonacci, C., Buch, A., Yang, L., Beal, M.F., Surmeier, D.J., Kordower, J.H., Tabar, V., Studer, L., 2011. Dopamine neurons derived from human es cells efficiently engraft in animal models of Parkinson's disease. Nature 480, 547–551. https://doi.org/10.1038/nature10648.

Lindvall, O., Brundin, P., Widner, H., Rehncrona, S., Gustavii, B., Frackowiak, R., Leenders, K.L., Sawle, G., Rothwell, J.C., Marsden, C.D., 1990. Grafts of fetal dopamine neurons survive and improve motor function in Parkinson's disease. Science (80-.) 247, 574–577.

Lindvall, O., Rehncrona, S., Brundin, P., Gustavii, B., Astedt, B., Widner, H., Lindholm, T., Björklund, A., Leenders, K.L., Rothwell, J.C., Frackowiak, R., Marsden, D., Johnels, B., Steg, G., Freedman, R., Hoffer, B.J., Seiger, A., Bygdeman, M., Strömberg, I., Olson, L., 1989. Human fetal dopamine neurons grafted into the striatum in two patients with severe Parkinson's disease. A detailed account of methodology and a 6-month follow-up. Arch. Neurol. 46, 615–631.

Lindvall, O., Widner, H., Rehncrona, S., Brundin, P., Odin, P., Gustavii, B., Frackowiak, R., Leenders, K.L., Sawle, G., Rothwell, J.C., 1992. Transplantation of fetal dopamine neurons in Parkinson's disease: one-year clinical and neurophysiological observations in two patients with putaminal implants. Ann. Neurol. 31, 155–165. https://doi.org/10.1002/ana.410310206.

Miyamoto, Y., Ikeuchi, M., Noguchi, N., Hayashi, S., 2018. Long-term cryopreservation of human and other mammalian cells at −80°C for 8 years. Cell Med 10, 2155179017733148.

McRitchie, D.A., Hardman, C.D., Halliday, G.M., 1996. Cytoarchitectural distribution of calcium binding proteins in midbrain dopaminergic regions of rats and humans. J. Comp. Neurol 364, 121–150.

Renier, N., Adams, E.L., Kirst, C., Wu, Z., Azevedo, R., Kohl, J., Autry, A.E., Kadiri, L., Umadevi Venkataraju, K., Zhou, Y., Wang, V.X., Tang, C.Y., Olsen, O., Dulac, C., Osten, P., Tessier-Lavigne, M., 2016. Mapping of brain activity by automated volume analysis of immediate early genes. Cell 165, 1789–1802. https://doi.org/10.1016/j.cell.2016.05.007.

Renier, N., Wu, Z., Simon, D.J., Yang, J., Ariel, P., Tessier-Lavigne, M., 2014. iDISCO: a simple, rapid method to immunolabel large tissue samples for volume imaging. Cell 159, 896–910. https://doi.org/10.1016/j.cell.2014.10.010.

Rienzi, L., Romano, S., Albricci, L., Maggiulli, R., Capalbo, A., Baroni, E., Colamaria, S., Sapienza, F., Ubaldi, F., 2010. Embryo development of fresh "versus" vitrified metaphase II oocytes after ICSI: a prospective randomized sibling-oocyte study. Hum. Reprod. 25, 66–73. https://doi.org/10.1093/humrep/dep346.

Sawle, G.V., Bloomfield, P.M., Björklund, A., Brooks, D.J., Brundin, P., Leenders, K.L., Lindvall, O., Marsden, C.D., Rehncrona, S., Widner, H., 1992. Transplantation of fetal dopamine neurons in Parkinson's disease: pet [18F]6-L-fluorodopa studies in two patients with putaminal implants. Ann. Neurol. 31, 166–173. https://doi.org/10.1002/ana.410310207.

Steinbeck, J.A., Choi, S.J., Mrejeru, A., Ganat, Y., Deisseroth, K., Sulzer, D., Mosharov, E.V., Studer, L., 2015. Optogenetics enables functional analysis of human embryonic stem cell-derived grafts in a Parkinson's disease model. Nat. Biotechnol. 33, 204–209. https://doi.org/10.1038/nbt.3124.

Steinbeck, J.A., Studer, L., 2015. Moving stem cells to the clinic: potential and limitations for brain repair. Neuron 86, 187–206. https://doi.org/10.1016/j.neuron.2015.03.002.

Studer, L., 2017. Strategies for bringing stem cell-derived dopamine neurons to the clinic-The NYSTEM trial. Prog Brain Res 230, 191–212. https://doi.org/10.1016/bs.pbr.2017.02.008.

Sundberg, M., Isacson, O., 2014. Advances in stem-cell–generated transplantation therapy for Parkinson's disease. Expert Opin Biol Ther 14, 437–453. https://doi.org/10.1517/14712598.2014.876986.

Tieu, K., 2011. A guide to neurotoxic animal models of Parkinson's disease. Cold Spring Harb Perspect Med 1, a009316.

Wakeman, D.R., Hiller, B.M., Marmion, D.J., McMahon, C.W., Corbett, G.T., Mangan, K.P., Ma, J., Little, L.E., Xie, Z., Perez-Rosello, T., Guzman, J.N., Surmeier, D.J., Kordower, J.H., 2017. Cryopreservation maintains functionality of human iPSC dopamine neurons and rescues Parkinsonian phenotypes in vivo. Stem Cell Rep. 9, 149–161. https://doi.org/10.1016/j.stemcr.2017.04.033.

Wong, K.G., Ryan, S.D., Ramnarine, K., Rosen, S.A., Mann, S.E., Kulick, A., De Stanchina, E., Müller, F.J., Kacmarczyk, T.J., Zhang, C., Betel, D., Tomishima, M.J., 2017. CryoPause: a new method to immediately initiate experiments after cryopreservation of pluripotent stem cells. Stem Cell Rep. 9, 355–365. https://doi.org/10.1016/j.stemcr.2017.05.010.

Yang, H., Acker, J.P., Cabuhat, M., McGann, L.E., 2003. Effects of incubation temperature and time after thawing on viability assessment of peripheral hematopoietic progenitor cells cryopreserved for transplantation. Bone Marrow Transpl. 32, 1021–1026. https://doi.org/10.1038/sj.bmt.1704247.